

ROBOT SENSOR CALIBRATION VIA NEURAL NETWORK AND PARTICLE SWARM OPTIMIZATION ENHANCED WITH CROSSOVER AND MUTATION

Dong-Yuan Ge, Xi-Fan Yao, Qing-He Yao, Hong Jin

Original scientific paper

In order to determine the position and orientation of an object in the wrist frame for robot, transform relation of hand-eye system should be estimated, which is described as rotational matrix and translational vector. A new approach integrating neural network and particle swarm optimization algorithm with crossover and mutation operation for robot sense calibration is proposed. First the neural network with rotational weight matrix is structured, where the weights are the elements of rotational part of homogeneous transform of the hand-eye system. Then the particle swarm optimization algorithm is integrated into the solving program, where the inertia weight factor and mutation probability are tuned self-adaptively according to the motion trajectory of particles in longitudinal direction and lateral direction. When the termination criterion is satisfied, the rotational matrix is obtained from the neural network's stable weights. Then the translational vector is solved, so the position and orientation of camera frame with respect to wrist frame is achieved. The proposed approach provides a new scheme for robot sense calibration with self-adaptive technique, which guarantees the orthogonality of solved rotational components of the homogeneous transform.

Keywords: crossover and mutation particle swarm optimization, lateral direction, longitudinal direction, neural network with rotational matrix, robot sensor calibration

Kalibracija senzora robota neuronskom mrežom i optimizacijom roja čestica poboljšana križanjem i mutacijom

Izvorni znanstveni članak

U cilju određivanja položaja i orientacije nekog predmeta u zglobu za robot, treba procijeniti odnos transformacije sustava ruka-oko, što se opisuje kao rotacijska matrica i vektor translacije. Predlaže se novi pristup koji integrira neuronsku mrežu i algoritam optimizacije roja čestica s operacijom križanja i mutacije za kalibraciju osjećaja robota. Najprije se strukturira neuronska mreža s matricom rotacijske težine gdje su težine elementi rotacijskog dijela homogenog prijenosa sustava ruka-oko. Tada se algoritam optimalizacije roja čestica integrira u program rješavanja, gdje se faktori težine inercije i vjerojatnosti mutacije sami podešavaju prema putanji gibanja čestica u longitudinalnom pravcu i lateralnom pravcu. Kad je zadovoljen kriterij terminacije, rotaciona matrica se dobiva iz nepromjenljivih težina neuronske mreže. Tada se rješava vektor translacije i postiže se položaj i orientacija slike s kamere u odnosu na sliku sa zgloba. Predloženi pristup pruža novu šemu za kalibraciju robota tehnikom samo-adaptacije, što garantira ortogonalnost riješenih rotacijskih komponenti homogenog transforma.

Ključne riječi: kalibracija senzora robota, lateralni pravac, longitudinalni pravac, neuronska mreža s rotacijskom matricom, optimalizacija roja čestica križanjem i mutacijom

1 Introduction

The machine vision is widely used in robots, such as explosive ordnance disposal (EOD) robot, welding robot, assembly robot and so on. Much research has been done on using a sensor to locate a work-piece, and the three-dimensional position and orientation of a work-piece can be estimated by monocular vision, stereo vision, dense/sparse range sensing and so on. Monocular vision locates an object using a single view, and the object dimensions are assumed to be known a priori [1, 2]. Stereo vision uses two cameras instead of one so that the range information of feature points can be estimated [3, 4]. A dense range sensor scans a region of the world and there are as many sensed points as its resolution allows [5, 6, 7]. A sparse range sensor only scans a few points, and if the sensed points are not sufficient to locate the work piece, additional points will be sensed [8, 9, 10]. Tactile sensing is similar to sparse range sensing to obtain the same information of the sensed points [9, 10]. As for the 6 degree of freedom robot, if the sensor is mounted on the fifth link of the robot, its motion will be limited to 5 degree of freedom. Once the sensor position and orientation relative to the last link is found, it is straightforward to find the sensor position and orientation relation to other links with encoder readings and link specification, so that the position and orientation of work-pieces in the wrist frame for a robot can be determined with machine vision.

While the transform relation of camera frame with respect to wrist frame is estimated, the direct measurements are difficult, because there may be obstacles to obstruct the measurement path, the points of interests may be inside a solid and be unreachable, and the coordinate frames may differ in their orientations. On the other hand the camera frame is unreachable because its origin is at the focal point, inside the camera. Instead of direct measurement, we can compute the camera position by displacing the robot and observing the changes in the sensor frame. This method works for any sensors capable of finding the 3-dimensional position and orientation of an object. There are many researchers working on the hand-eye calibration, for example, Shiu and Park et al. solved homogenous transform equation to achieve the calibration of wrist-mounted robotic sensors with least square method by solving homogeneous transform equations of the form $AX=XB$ [11-13]. Yang et al. presented a new wrist-mounted robotic sensor calibration approach which utilized nominal rotation for camera frame to make rotation transform into translation, thus two translation motions and one rotation motion are needed, and only two feature points in the scene are required [14]. Y. Motai et al. utilized the Broyden-Fletcher-Goldfarb-Shanno optimization algorithm to obtain a solution which minimized the objective function $f(q) = \|e_2^T R \cdot e R - h_2^T R \cdot h_2\|_2$ [15]. Zhang et al. adopted Kronecker product and particle swarm optimization to achieve the solution of rotation and translation

simultaneously [16]. M. X. Li dealt with the kinematics calibration for an active head-eye system by non-linear optimization solution for the rotational components of the head-eye relation [17]. F. Dornaika and R. Horaud proposed a non-linear constrained minimization optimization method to solve the rotational and transformational components of the hand-eye system's homogeneous transform simultaneously [18]. There is a research report on calibration of wrist-mounted robot sensors by integrating a neural network with basic genetic algorithm. Although it may be the first report on hand-eye calibration by neural network with orthogonal matrix, however the weight vectors of the neural network should be transformed according to the cross product principle to get orthogonal vectors and to form rotational matrix, and it is complicated and miscellaneous for computing [19]. Based on the above researches, in the paper we proposed a novel approach to realize the robot sensor calibration, according to the requirements of hand-eye calibration for a manipulator. Our contributions are in the following: first a neural network with rotational weights matrix is structured, where the weights matrices are the rotational components of the eye-in-hand's homogeneous transform; then a novel approach i.e. particle swarm optimization with enhancement of crossover and mutation (abbr. as PSOECM) is proposed, where motion trajectories of particles are analysed in longitudinal direction and lateral direction, so the inertia weights of particle swarm optimization (abbr. as PSO) and mutation probability are tuned self-adaptively.

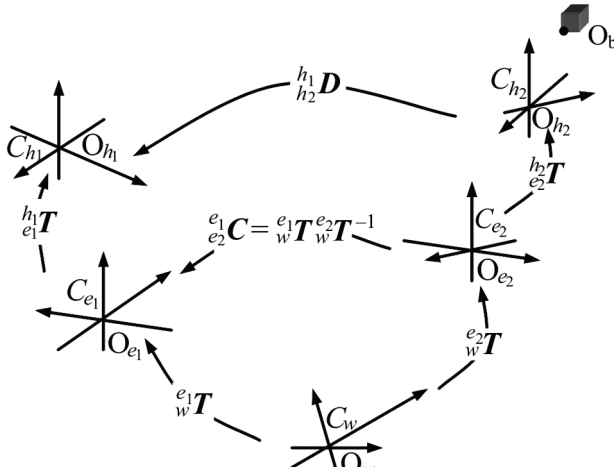


Figure 1 Machine vision system of manipulator

The paper is organized as follows. First the hand-eye relation i.e. the position and orientation of a wrist-mounted sensor with respect to the robot wrist frame is analysed and inferred in the next section. Then some properties of rotational matrix are explored, and the general solution algorithm to the rotational components of a solvable homogeneous transform equation of the form $\frac{e_1}{e_2} \mathbf{C} \cdot {}^e \mathbf{T} = {}^e \mathbf{T} \cdot {}^{h_1} \mathbf{D}$ is discussed in Section 3. In Section 4, hybrid neural network and particle swarm optimization is proposed, where the neural network is designed with rotational weight matrix, and the particle swarm optimization algorithm with crossover and mutation operation is adopted. Then the robot sensor calibration experiment is demonstrated and the position and

orientation of camera frame with respect to wrist frame are estimated with the proposed approach in Section 5. Finally, conclusions, further work and direction in this field are given in Section 6.

2 Hand-eye relation and homogeneous transform model

As shown in Fig. 1, C_{h1} and C_{h2} are the wrist frame before and after motion respectively, C_{e1} and C_{e2} are the camera frame before and after motion respectively; C_w is the world frame. The position and orientation of the camera frame with respect to the wrist frame is invariant before and after motion; and we let ${}^e \mathbf{T}_{e1} = {}^{h_1} \mathbf{T} = {}^{h_2} \mathbf{T}$. Assume the relations of the camera frame C_{e1} and C_{e2} with respect to the world frame C_w are ${}^w \mathbf{T}^1$ and ${}^w \mathbf{T}^2$; thus the relation of C_{e2} with respect to C_{e1} is ${}^{e_2} \mathbf{C} = {}^w \mathbf{T}^1 \cdot {}^w \mathbf{T}^{-1}$. The position and orientation of the wrist frame C_{h2} with respect to C_{h1} can be read from the manipulator's controller, which is described as ${}^{h_2} \mathbf{D}$. Thus the transform relations of C_{e1} , C_{h1} , C_{e2} and C_{h2} are described as follows,

$${}^{e_2} \mathbf{C} \cdot {}^e \mathbf{T} = {}^e \mathbf{T} \cdot {}^{h_2} \mathbf{D}. \quad (1)$$

Eq. (1) is the homogeneous transform equation for hand-eye system of manipulator. With rotational matrix \mathbf{R} and translational vector \mathbf{P} , Eq. (1) can be rewritten as follows

$$\begin{bmatrix} {}^{e_1} \mathbf{R} & {}^{e_1} \mathbf{P}_{oe2} \\ {}^{e_2} \mathbf{R} & {}^{e_2} \mathbf{P}_{oe2} \\ \mathbf{0} & 1 \end{bmatrix} \cdot \begin{bmatrix} {}^e \mathbf{R} & {}^e \mathbf{P}_h \\ {}^h \mathbf{R} & {}^h \mathbf{P}_h \\ \mathbf{0} & 1 \end{bmatrix} = \begin{bmatrix} {}^e \mathbf{R} & {}^e \mathbf{P}_h \\ {}^{h_2} \mathbf{R} & {}^{h_2} \mathbf{P}_{oh2} \\ \mathbf{0} & 1 \end{bmatrix}, \quad (2)$$

where $\mathbf{0}$ is a row of 3 zeros. By multiplying out and equating the first row of Eq. (2), we have,

$${}^{e_2} \mathbf{R} \cdot {}^e \mathbf{R} = {}^e \mathbf{R} \cdot {}^{h_2} \mathbf{R}, \quad (3)$$

$${}^{e_2} \mathbf{R} \cdot {}^e \mathbf{P}_h + {}^{e_2} \mathbf{P}_{oe2} = {}^e \mathbf{R} \cdot {}^{h_2} \mathbf{P}_{oh2} + {}^e \mathbf{P}_h. \quad (4)$$

3 Rotational matrix and solving conditions for uniqueness

Rotational matrix, such as ${}^e \mathbf{R}$ can be expressed as a rotation of angle θ around an axis $\mathbf{k} = k_x \vec{i} + k_y \vec{j} + k_z \vec{k}$, that is [20]

$$\mathbf{R}(\mathbf{k}, \theta) = e^{\mathbf{k} \times \theta}, \quad (5)$$

where $\mathbf{k} \times$ is a skew-symmetric matrix, that is

$$\mathbf{k} \times = \begin{bmatrix} 0 & -k_z & k_y \\ k_z & 0 & -k_x \\ -k_y & k_x & 0 \end{bmatrix}.$$

Fisher has shown that the eigen-values of $\mathbf{k} \times$ are $-j, j$ and 0, and these eigen-values are distinct, so $\mathbf{k} \times$ in Eq. (5) can be diagonalized. Let it be the diagonalizing matrix whose columns contain independent eigen-vectors, so the

skew-symmetric matrix can be rewritten as follows,

$$\mathbf{k}_x = \mathbf{E} \begin{bmatrix} -j & 0 & 0 \\ 0 & j & 0 \\ 0 & 0 & 0 \end{bmatrix} \mathbf{E}. \quad (6)$$

$$\begin{aligned} e^{\mathbf{k}_x \theta} &= \sum_{i=0}^{\infty} \frac{(\mathbf{k}_x \theta)^i}{i!} = \\ &= \mathbf{I}_3 + \left(\frac{\theta}{1!} \mathbf{E} \begin{bmatrix} -j & 0 & 0 \\ 0 & j & 0 \\ 0 & 0 & 0 \end{bmatrix} \mathbf{E}^{-1} - \frac{\theta^3}{3!} \mathbf{E} \begin{bmatrix} -j & 0 & 0 \\ 0 & j & 0 \\ 0 & 0 & 0 \end{bmatrix} \mathbf{E}^{-1} + \dots + (-1)^{n-1} \frac{\theta^{2n-1}}{(2n-1)!} \mathbf{E} \begin{bmatrix} -j & 0 & 0 \\ 0 & j & 0 \\ 0 & 0 & 0 \end{bmatrix} \mathbf{E}^{-1} \right) + \\ &\quad + \left(-\frac{\theta^2}{2!} \mathbf{E} \begin{bmatrix} 1 & 0 & 0 \\ 0 & 1 & 0 \\ 0 & 0 & 0 \end{bmatrix} \mathbf{E}^{-1} + \frac{\theta^4}{4!} \mathbf{E} \begin{bmatrix} 1 & 0 & 0 \\ 0 & 1 & 0 \\ 0 & 0 & 0 \end{bmatrix} \mathbf{E}^{-1} - \dots + (-1)^{n-1} \frac{\theta^{2n}}{(2n)!} \mathbf{E} \begin{bmatrix} 1 & 0 & 0 \\ 0 & 1 & 0 \\ 0 & 0 & 0 \end{bmatrix} \mathbf{E}^{-1} \right). \end{aligned} \quad (7)$$

According to the Taylor's expansion of $\sin \theta$ and $\cos \theta$, by simplifying we have

$$e^{\mathbf{k}_x \theta} = \mathbf{E} \begin{bmatrix} e^{-j\theta} & 0 & 0 \\ 0 & e^{j\theta} & 0 \\ 0 & 0 & 1 \end{bmatrix} \mathbf{E}^{-1}, \quad (8)$$

where $e^{-j\theta}$, $e^{j\theta}$ and 1 are eigen-values of h_R , and eigenvector (the third column of \mathbf{E}) of h_R corresponding to eigen-value of constant 1 is rotational axis \mathbf{k} .

According to Eq. (3) we have ${}^{e1}_2 \mathbf{R} = {}^e_R \cdot {}^{h1}_2 \mathbf{R} \cdot {}^h_R^{-1}$, so ${}^{e1}_2 \mathbf{R}$ and ${}^{h1}_2 \mathbf{R}$ are similar matrices, and their rotational angles are equal. Let it be θ , and assume \mathbf{k}_e and \mathbf{k}_h are their rotational axes, thus

$$\mathbf{R}(\mathbf{k}_e, \theta) = ({}^h_R \mathbf{E}) \begin{bmatrix} e^{-j\theta} & 0 & 0 \\ 0 & e^{j\theta} & 0 \\ 0 & 0 & 1 \end{bmatrix} ({}^h_R \mathbf{E})^{-1}, \quad (9)$$

where \mathbf{k}_h and \mathbf{k}_e axes are the 3rd column of \mathbf{E} and ${}^h_R \mathbf{E}$ respectively, thus we have

$$\mathbf{k}_e = {}^h_R \mathbf{R} \mathbf{k}_h. \quad (10)$$

From the above we know that if h_R is a solution to Eq. (3), which must meet $\mathbf{k}_e = {}^h_R \mathbf{R} \mathbf{k}_h$; in turn, if h_R meets $\mathbf{k}_e = {}^h_R \mathbf{R} \mathbf{k}_h$, which is a solution to Eq. (3). That means that any h_R meets Eq. (3) can rotate \mathbf{k}_h to \mathbf{k}_e .

Lemma 1: If \mathbf{R} is a rotational matrix and $\mathbf{R} \text{rot}(\mathbf{k}_i, \theta) = \text{rot}(\mathbf{k}_i, \theta) \mathbf{R}$, and $\theta \neq 0$ (or π), then $\mathbf{R} = \text{rot}(\mathbf{k}_i, \beta)$, where β is arbitrary.

According to Eq. (3), there must exist some rotational matrix \mathbf{R}' meet

$${}^{e1}_2 \mathbf{R} \cdot \mathbf{R}' = \mathbf{R}' \cdot {}^{h1}_2 \mathbf{R}. \quad (11)$$

According to Taylor's expansion we have Eq. (7).

Assume \mathbf{R}_1 is a particular solution to Eq. (3), so ${}^{h1}_2 \mathbf{R} = \mathbf{R}_1^{-1} \cdot {}^{e1}_2 \mathbf{R} \mathbf{R}_1$. Plugging it into Eq. (11), we have

$$\mathbf{R}'^{-1} \cdot {}^{e1}_2 \mathbf{R} \cdot \mathbf{R}' = \mathbf{R}_1^{-1} \cdot {}^{e1}_2 \mathbf{R} \cdot \mathbf{R}_1. \quad (12)$$

Rewrite ${}^{e1}_2 \mathbf{R}$ as $\text{rot}(\mathbf{k}_e, \theta)$ and rearrange, Eq. (12) can be rewritten as follows,

$$\text{rot}(\mathbf{k}_e, \theta) \cdot \mathbf{R}' \cdot \mathbf{R}_1^{-1} = \mathbf{R}' \cdot \mathbf{R}_1^{-1} \cdot \text{rot}(\mathbf{k}_e, \theta). \quad (13)$$

Thus $\text{rot}(\mathbf{k}_e, \theta)$ and $\mathbf{R}' \cdot \mathbf{R}_1^{-1}$ are commutative. If the rotational angle θ is neither 0 nor π . From lemma 1, the rotational axis of $\mathbf{R}' \cdot \mathbf{R}_1^{-1}$ must be parallel or anti-parallel to \mathbf{k}_e . So there must exist a β such that $\mathbf{R}' \cdot \mathbf{R}_1^{-1} = \text{Rot}(\mathbf{k}_e, \beta)$. Thus the general solution to ${}^{e1}_2 \mathbf{R} \cdot {}^e_R = {}^e_R \cdot {}^{h1}_2 \mathbf{R}$ can be obtained as follows,

$$\mathbf{R} = \text{rot}(\mathbf{k}_e, \beta) \mathbf{R}_1, \quad (14)$$

where \mathbf{R}_1 is a particular solution to the Eq. (3), and β is an arbitrary angle. Thus the unique solution cannot be obtained for the Eq. (3) as there is a freedom degree.

While the translational vector ${}^e P_h$ is solved, Eq. (4) can be written as

$$({}^{e1}_2 \mathbf{R} - \mathbf{I}) \cdot {}^e P_h = {}^e R \cdot {}^{h1} P_{oh2} - {}^{e1} P_{oe2}. \quad (15)$$

According to the properties of the eigen-values and eigen vectors of rotational matrix, we have

$${}^{e1}_2 \mathbf{R} - \mathbf{I} = \mathbf{E} \begin{bmatrix} e^{-j\theta} - 1 & 0 & 0 \\ 0 & e^{j\theta} - 1 & 0 \\ 0 & 0 & 0 \end{bmatrix} \mathbf{E}. \quad (16)$$

From Eq. (16) we know that the rank of $({}^{e1}_2 \mathbf{R} - \mathbf{I})$ is 2, so there may be no solution or there are infinite number of solutions to ${}^e P_h$. The first case is ruled out since the physical system guarantees the existence of a solution.

The solution must exist and consist of all the vectors in the null space of $\begin{pmatrix} {}^e_2\mathbf{R} - \mathbf{I} \end{pmatrix}$ translated by a particular solution to Eq. (15). The null space of $\begin{pmatrix} {}^e_2\mathbf{R} - \mathbf{I} \end{pmatrix}$ has a dimension of 3-rank $\begin{pmatrix} {}^e_2\mathbf{R} - \mathbf{I} \end{pmatrix}$, so there is one freedom degree for solution to be determined.

As there are a rotational freedom degree and a translational freedom degree while the ${}^e_h\mathbf{R}$ and ${}^e\mathbf{P}_h$ are solved according to Eqs. (10) and (15), in order to solve the ${}^e_h\mathbf{T}$ uniquely, it is necessary to let manipulator two movements and form a system of two homogeneous transform equations of the form: ${}^e_2\mathbf{C} \cdot {}^e_h\mathbf{T} = {}^e_h\mathbf{T} \cdot {}^h_2\mathbf{D}$, and

$$\mathbf{R}(\mathbf{k}, \theta) = \begin{bmatrix} k_x k_x (1 - \cos \theta) + \cos \theta & k_y k_x (1 - \cos \theta) - k_z \sin \theta & k_z k_x (1 - \cos \theta) + k_y \sin \theta \\ k_x k_y (1 - \cos \theta) + k_z \sin \theta & k_y k_y (1 - \cos \theta) + \cos \theta & k_z k_y (1 - \cos \theta) - k_x \sin \theta \\ k_x k_z (1 - \cos \theta) - k_y \sin \theta & k_y k_z (1 - \cos \theta) + k_x \sin \theta & k_z k_z (1 - \cos \theta) + \cos \theta \end{bmatrix}$$

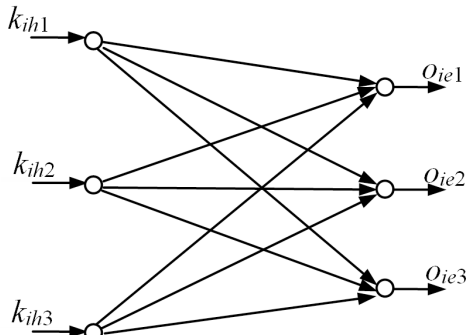


Figure 2 Neural network with rotational matrix

According to the Eq. (10), i.e. $\mathbf{k}_e = {}^e_h\mathbf{R} \cdot \mathbf{k}_h$, a neural network with rotational matrix is structured and shown in Fig. 2. Let weight matrix $\mathbf{R} = [\mathbf{n}, \mathbf{o}, \mathbf{a}]$, where normal vector $\mathbf{n} = [r_{11}, r_{21}, r_{31}]^T$, orientation vector $\mathbf{o} = [r_{12}, r_{22}, r_{32}]^T$, and approach vector $\mathbf{a} = [r_{13}, r_{23}, r_{33}]^T$. The inputs of the network are elements of $\mathbf{k}_{ih} = [k_{ih1}, k_{ih2}, k_{ih3}]^T$, and the outputs can be obtained through forward channel computing, which constitute the vector $\mathbf{o}_{ie} = [o_{ie1}, o_{ie2}, o_{ie3}]^T$, that is $\mathbf{o}_{ie} = {}^e\mathbf{R}\mathbf{k}_{ih}$. And the expected values of the network are the elements of rotational axis $\mathbf{k}_{ie} = [k_{ie1}, k_{ie2}, k_{ie3}]^T$. In the light of the solving objective, let the performance index of system be

$$E_i = \frac{1}{2} \sum_{j=1}^3 (k_{iej} - o_{iej})^2, \quad i = 1, 2, \dots, 48.$$

Thus if the neural network comes to the global optimization balance position, the rotational components of the homogeneous transform of the eye-in-hand system can be estimated from the network weights as Eq. (10) is transformed into Fig. 2 [21, 22].

4.2 Integration with crossover and mutation particle swarm optimization algorithm

While the rotational matrix of hand-eye system is fitted, we integrate the neural network with particle

${}^e_3\mathbf{C} \cdot {}^e_h\mathbf{T} = {}^e_h\mathbf{T} \cdot {}^h_3\mathbf{D}$. So a closed-form solution to the eye-in-hand system can be obtained.

4 Solving with combination of neural network and particle swarm optimization

4.1 Neural network structured with rotational weight matrix

Rotational weight matrix such as ${}^e_h\mathbf{R}$ has 9 unknown parameters, however only 3 parameters of them are independent, which can be expressed as a rotation by angle θ about arbitrary axis $\mathbf{k} = k_x \vec{i} + k_y \vec{j} + k_z \vec{k}$, that is

swarm optimization (PSO) algorithm, which is a stochastic optimization algorithm. The swarm consists of 48 particles, which move around in a 3 dimensional searching space at variant velocities according to individual experience and swarm experience, and adjust their velocities and positions dynamically. The elements of particles' position are k_x , k_y and θ ; The objective function is the performance index of the structured neural network; the search space of k_x and k_y is $[-1, 1]$; and the search space of θ is $[0; 3, 14]$. In the iteration, if

$k_x^2 + k_y^2 \leq 1$, and $k_z = \pm \sqrt{1 - k_x^2 - k_y^2}$. As for positive or negative, it is chosen according to which one makes performance index smaller; else let $k_z = \text{rand}(.)$, then the rotational axis is normalized to form a unit vector; and the above operation can be taken as constrained mutation operation for the rotational axis, which don't influence the particles' evolution direction to optimization solutions basically. Each particle is composed of three elements such as k_x , k_y and θ is taken as a potential solution to a problem. Assume the position of the i^{th} particle is represented as $\mathbf{x}_i = (x_{i1}, x_{i2}, x_{i3})$, the best previous encountered position of the i^{th} particle is denoted its individual best position $\mathbf{p}_{li} = (p_{i1}, p_{i2}, p_{i3})$, its value called p_{best} is the smallest value of i^{th} particle by far. The best value of all individual p_{best} values is denoted the global best position $\mathbf{p}_g = (g_{i1}, g_{i2}, g_{i3})$ up to now, and called g_{best} ; a velocity along each dimension is represented as $\mathbf{v}_i = (v_{i1}, v_{i2}, v_{i3})$. The velocity updating equation is formulated as follows,

$$\mathbf{v}_i(t+1) = \omega \mathbf{v}_i(t) + c_1 r_1 (\mathbf{p}_{li} \otimes \mathbf{x}_i(t)) + c_2 r_2 (\mathbf{p}_g(t) \otimes \mathbf{x}_i(t)). \quad (18)$$

where \otimes denotes crossover operation, and the velocity vector has three components. The first one is the inertia term which keeps the particle move to next position, and plays the role of balancing the global and local searches. A large inertia weight facilitates a global search while a small inertia weight favor local search with high ability. The second one is the cognitive component, which is its

own thoughts and experience. The third one is the social component, which represents the messages shared all particles swarm and guide to the global best. c_1 and c_2 are the two acceleration coefficients, and are both set to values of 2,0 in the experiment. r_1 and r_2 are random numbers in the range of [0, 1] [23]. The crossover probability for velocity updating is 1. And the crossover operation is carried out with arithmetic crossover that produces two complimentary linear combinations of the parents: that is $p_{li}(t) \otimes x_i(t) = r_1 p_{li}(t) + (1 - r_1) x_i(t)$, $p_g(t) \otimes x_i(t) = (1 - r_1) p_g(t) + r_1 x_i(t)$, and where $r_1 \subset [0; 1]$, is a random number.

Then the position of particles is updated as follows,

$$\mathbf{x}_i(t+1) = \mathbf{x}_i(t) + \mathbf{v}_i(t+1). \quad (19)$$

At the same time, a mutation operation is introduced into the position adjustment, which services for introducing a noise into the information of a particle, so that variety of the swarm can be guaranteed. One variable of position vector is selected randomly, so the non-uniform mutation operation for the selected variable is dealt with according to p_m as follows,

$$x_m(t) = \begin{cases} x_m(t-1) + (b_i - x_m(t-1))f(t) & \text{if } 0 \leq \lambda_1 < 0,5 \\ x_m(t-1) - (x_m(t-1) - a_i)f(t) & \text{if } 0,5 < \lambda_1 \leq 1 \end{cases}. \quad (20)$$

where function $f(t) = \lambda_2 \left(1 - \frac{t}{T}\right)^b$, and shape parameter $b = 2$, which determines the non-uniform degree of the operation. λ_1 , λ_2 are uniform random numbers between (0, 1); $x_m(t)$ and $x_m(t-1)$ are the m^{th} variables of the vector $\mathbf{x}_i(t)$ at the t^{th} generation and $(t-1)^{\text{th}}$ generation, a_i and b_i are the lower and upper bound of $x_m(t)$, which are set 0 and 1 in the experiment; t is the current generation, and T is the maximum number of generations.

4.3 Parameters tuning of particle swarm optimization

4.3.1 Evolution speed factor and square deviation factor of particles

1) Evolution speed factor

In longitudinal direction, the direction and degree of evolution can be forecasted by individual evolution speed factor, as the derivative term can forecast signal variations in a proportional-integral-derivative (PID) controller. The performance of the particle evolution process of the PSO is measured with evolution speed factor, which is expressed as follows,

$$e = \frac{1}{N} \sum_{i=1}^N \left(\min \left(1, \frac{E_i(t-1) - E_i(t)}{E_i(t-1) + r_3 \varepsilon_1} \right) \right), \quad (21)$$

where $E_i(t-1)$ and $E_i(t)$ are objective function of system at the $(t-1)^{\text{th}}$ and t^{th} generation for i^{th} particle, which can be obtained from the performance index of the neural network; $N = 48$, which is the number of

population; r_3 is random number between (0, 1), ε_1 is a small constant nearly approximate to zero taken as an offset bias value, in case $E_i(t-1)$ equals to zero; in this experiment, let $\varepsilon_1 = 1 \times 10^{-14}$. And $0 < e \leq 1$; the smaller the e is, the slower the evolution speed is. While $e = 0$, the algorithm stagnates or the optimal solution is found [24].

2) Square deviation factor of particles

In lateral direction, if the particles' diversity decreases too soon during the iteration, the algorithm may not search the global optimization solution for the system. In order to represent the particles' diversity, a so-called square deviation factor of particles is introduced, which describes the particles' distribution. In the experiment the square deviation of particles is given by the following equation by,

$$\sigma_t = \frac{1}{N} \sum_{i=1}^N (E(\mathbf{x}_i(t)) - E_v)^2, \quad (22)$$

where E_v is the average number of particles' objective function $E(\mathbf{x}_i(t))$, i.e. $E_v = \frac{1}{N} \sum_{i=1}^N E(\mathbf{x}_i(t))$. In view of normalization processing, the square deviation factor of the particles can be written as follows,

$$\psi_t = \frac{\sigma_t}{\max(\sigma_1, \sigma_2, \dots, \sigma_t)}. \quad (23)$$

It is obvious that $0 \leq \psi_t < 1$; and the bigger the ψ_t is, the more the diversity of the particles is [25].

4.3.2 Self-adaptive tuning of inertia weight and mutation probability

According to the motion trajectory characteristic of particles, the suitable coefficient ω can find the global optimum within a reasonable number of iterations. If the evolution speed of individuals is fast, the algorithm can search optimization solution at large scope. On the other hand, if the square deviation factor of individuals is small, the algorithm will be trapped in local optimization position easily [26]. In order to obtain the global optimization solution we proposed an innovative approach. According to the characteristic of the individual's motion trajectory from the lateral direction and longitudinal direction, at the beginning, inertia weight factor ω and mutation probability p_m should increase along with the increasing of gathering degree of individuals, and increase along with decreasing of individuals evolution speed accordingly. On the other hand, to guarantee the convergence of algorithm, the inertia weight factor ω and mutation probability p_m should adopt smaller value for particles with higher fitness degree while the iteration achieved into the neighbourhood of the global optimization position. ω and p_m are modified dynamically as follows,

$$\omega = \omega_{e\omega} e^{-\frac{(e_t - 0.6)^2}{2 \times 0.38^2}} + \omega_{\sigma\omega} e^{-\frac{(\sigma_t - 0.14)^2}{2 \times 0.16^2}}, \quad (24)$$

$$p_m = \omega_{em} e^{-\frac{(e_t - 0.5)^2}{2 \times 0.64^2}} + \omega_{\sigma m} e^{-\frac{(\sigma_t - 0.15)^2}{2 \times 0.2^2}}, \quad (25)$$

where $\omega_{e\omega}$, ω_{em} , $\omega_{\sigma\omega}$ and $\omega_{\sigma m}$ are the coefficients of evolution speed factor and square deviation factor of particles; their ranges are defined as $0 < \omega_{e\omega}, \omega_{em} < 1$, $0 < \omega_{\sigma\omega}, \omega_{\sigma m} < 1$. In the experiment, let $\omega_{e\omega} = 0.8$, $\omega_{em} = 0.04$, $\omega_{\sigma\omega} = 0.5$ and $\omega_{\sigma m} = 0.05$. Self-adaptive tunings of inertia weight factor ω and mutation probability p_m are shown in Fig. 3, where SDF denotes the square deviation factor of particles, and ESF denotes the evolution speed factor. As for the inertia weight factor, From the Eq. (24) and Fig. 3, we can see that the evolution speed factor play larger influence in large value, i.e. at larger evolution velocity of particle. At the same time, in order to make particles to search the optimization solution at larger scope, the inertia weight factor increase along evolution process until the evolution speed factor is smaller 0,6 at the initial phase of iteration.

On the other hand, when the program process at the state that the square deviation factor of particles is at the neighbourhood of 0,14, the square deviation factor play larger role for inertia weight factor, which decrease sharply so as to improve the diversity of particles. And when the program come to the neighbourhood of global optimization solution, in order to guarantee the convergence of algorithm, let the inertia weight factor decrease sharply while the square deviation factor of particles is smaller, in this experiment, when the $\sigma_t < 0.14$. As can be seen from Fig. 3 and Eq. (25), it is similar for the self-adaptive adjusting of mutation probability p_m .

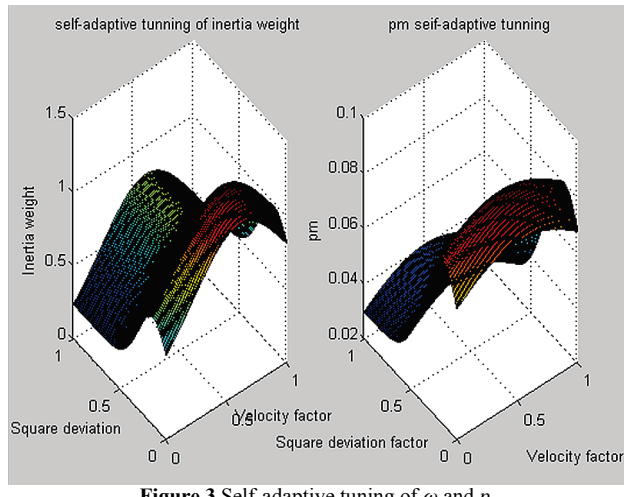


Figure 3 Self-adaptive tuning of ω and p_m

4.4 Chart-flow of solving program

The implementation steps of solving program is shown as follows:

Step 1. Initializing the position and velocity vector of each particle randomly, where the rotational axis is initialized with 3 random numbers, then to obtained unit

vector by normalized processing. The rotational angle is initialized with a random function, which is between 0 and 3,14; so the rotational axis and rotational angle consist of a particle's position, which is a vector with 3 elements; and other 47 particles' positions are initialized similarly. The other constant parameters are set as follows: acceleration coefficients $c_1=c_2=2$, the iteration is 320, population size is 48, the offset bias value $\varepsilon_1=1\times 10^{-14}$.

Step 2. Calculating the fitness value of each particle, which is obtained from performance index of the neural network, that is $f(\mathbf{x}_i)=\frac{1}{E_i - r_4 \times 1 \times 10^{-14}}$, where the E_i is performance index of the neural network, r_4 is random number between (0, 1).

Step 3. For each particle, comparing its fitness value $f(\mathbf{x}_i)$ with the value of fitness individual experienced best position p_{li} , if $f(\mathbf{x}_i) > p_{li}$, let $p_{besti} = f(\mathbf{x}_i)$ and $p_{li} = \mathbf{x}_i$. And comparing its fitness value with the global best p_{gbest} position's, if $f(\mathbf{x}_i) > p_g$, let $p_g = f(\mathbf{x}_i)$ and $p_g = \mathbf{x}_i$.

Step 4. Computing the evolution speed factor and square deviation of fitness according to the Eq. (24) and (25), then obtained the inertia weight ω and the mutation probability p_m .

Step 5. Updating of the current particle's velocity and position according to the Eqs. (18) and (19).

Step 6. According to the mutation probability P_m , and generating a random number $r \in [0,1]$, if $r < p_m$, the mutation operator is carried on with Eq. (20); or go to Step 7.

Step 7. Setting iteration=iteration+1, if iteration<320, going back to Step 2, else, the best result will be obtained.

5 Calibration experiment and precision analysis

5.1 Hand-eye calibration experiment

The robot sensor calibration experiment is carried out in eye-in-hand system of robot, which consists of a 6-degree-of-freedom manipulators and a camera. As there are two freedom degrees to be determined while hT_w is solved according to Eq. (1), so let the manipulator move 3 times, ${}^{e1}C={}^{e1}T_w {}^{e2}T_w^{-1}$, ${}^{e2}C={}^{e2}T_w {}^{e3}T_w^{-1}$ and ${}^{e3}C={}^{e3}T_w {}^{e4}T_w^{-1}$ are obtained according to camera's extrinsic parameters ${}^{e1}T_w, {}^{e2}T_w, \dots, {}^{e4}T_w$, which are shown as follows [27 ÷ 29],

$${}^{e1}C = \begin{bmatrix} 0,9759 & -0,2149 & 0,0382 & -0,4203 \\ 0,2139 & 0,9765 & 0,0274 & 4,0629 \\ -0,0432 & -0,0186 & 0,9989 & 40,9565 \\ 0 & 0 & 0 & 1 \end{bmatrix},$$

$${}^{e2}C = \begin{bmatrix} 0,9468 & -0,2657 & 0,1813 & 46,7499 \\ 0,2629 & 0,9640 & 0,0397 & 28,7530 \\ -0,1853 & 0,0101 & 0,9826 & 76,4267 \\ 0 & 0 & 0 & 1 \end{bmatrix},$$

$$\begin{matrix} {}^{e3}\mathbf{C} \\ {}^{e4}\mathbf{C} \end{matrix} = \begin{bmatrix} 0,7568 & -0,6037 & 0,2508 & 49,6182 \\ 0,6536 & 0,6925 & -0,3054 & 60,6975 \\ 0,0107 & 0,3950 & 0,9186 & 49,3622 \\ 0 & 0 & 0 & 1 \end{bmatrix}.$$

$${}^e\mathbf{R} = \begin{bmatrix} -0,1574 & -0,3349 & 0,9290 \\ 0,9463 & -0,3201 & 0,0450 \\ 0,2823 & 0,8862 & 0,3673 \end{bmatrix}.$$

Their rotational axes are $\mathbf{K}_{e1} = [-0,1048, 0,1855, 0,9770]^T$, $\mathbf{K}_{e2} = [-0,0459, 0,5693, 0,8209]^T$, and $\mathbf{K}_{e3} = [0,4801, 0,1646, 0,8617]^T$; and their rotational angles are $12,6751^\circ, 18,7843^\circ$ and $46,8492^\circ$, respectively.

On the other hand, the relations of position and orientation of wrist frames at four positions, that is ${}^{h1}\mathbf{D}, {}^{h2}\mathbf{D}, {}^{h3}\mathbf{D}, {}^{h4}\mathbf{D}$ are obtained from the controller, we have

$$\begin{matrix} {}^{h1}\mathbf{D} \\ {}^{h2}\mathbf{D} \end{matrix} = \begin{bmatrix} 0,9803 & -0,0524 & 0,1905 & 22,3217 \\ 0,0709 & 0,9933 & 0,0915 & 31,8272 \\ -0,1844 & 0,1031 & 0,9774 & 13,6549 \\ 0 & 0 & 0 & 1 \end{bmatrix},$$

$$\begin{matrix} {}^{h2}\mathbf{D} \\ {}^{h3}\mathbf{D} \end{matrix} = \begin{bmatrix} 0,9795 & -0,0685 & 0,1896 & 47,6352 \\ 0,1144 & 0,9633 & -0,2428 & 29,6315 \\ -0,1660 & 0,2595 & 0,9514 & 81,6971 \\ 0 & 0 & 0 & 1 \end{bmatrix},$$

$$\begin{matrix} {}^{h3}\mathbf{D} \\ {}^{h4}\mathbf{D} \end{matrix} = \begin{bmatrix} 0,7136 & -0,5047 & 0,4859 & 43,6257 \\ 0,6195 & 0,7784 & -0,1013 & 12,3647 \\ -0,3271 & 0,3733 & 0,8681 & 72,2146 \\ 0 & 0 & 0 & 1 \end{bmatrix}.$$

Their rotational axes are $\mathbf{K}_{h1} = [0,4422, 0,8521, 0,2801]^T$, $\mathbf{K}_{h2} = [0,7823, 0,5539, 0,2850]^T$ and $\mathbf{K}_{h3} = [0,3236, 0,5545, 0,7667]^T$; and their rotational angles are $12,7103^\circ, 18,7251^\circ$ and $47,1532^\circ$ respectively.

In the experiment, according to the orthogonal vector characteristic, let $\mathbf{k}_{4e} = \mathbf{k}_{1e} \times \mathbf{k}_{2e}$, $\mathbf{k}_{5e} = \mathbf{k}_{2e} \times \mathbf{k}_{3e}$, $\mathbf{k}_{4h} = \mathbf{k}_{1h} \times \mathbf{k}_{2h}$, and $\mathbf{k}_{5h} = \mathbf{k}_{2h} \times \mathbf{k}_{3h}$. In the solving program, the input vectors are $\mathbf{k}_{1e}, \mathbf{k}_{2e}, \dots, \mathbf{k}_{5e}$, and their corresponding desired vectors are $\mathbf{k}_{1h}, \mathbf{k}_{2h}, \mathbf{k}_{3h}, \mathbf{k}_{4h}, \mathbf{k}_{5h}$ respectively. While the termination criterion is satisfied, a global extremum is obtained, that is the rotational angle θ is $123,7178^\circ$, and the rotational axis $\mathbf{k} = 0,5057\bar{i} + 0,3888\bar{j} + 0,7702\bar{k}$, i.e. the rotational matrix can be obtained according to the stable weights as follows,

Then in the light of least square method, the translational vector is obtained as follows,

$${}^e\mathbf{P}_h = [26,6562; 20,8910; 102,0396]^T.$$

If the traditional data processing approach such as least square method is adopted, the robot sensor calibration is achieved as follows [30],

$${}^e\mathbf{R} = \begin{bmatrix} -0,1531 & -0,3271 & 0,9049 \\ 0,9491 & -0,3098 & 0,0422 \\ 0,2866 & 0,8813 & 0,3669 \end{bmatrix},$$

$${}^e\mathbf{P}_h = [26,9997; 22,3209; 100,2951]^T.$$

5.2 Precision analysis of calibration

While precision analysis of eye-in-hand system is carried out, let $\mathbf{T}_{eri} = {}^{e(i+1)}\mathbf{C} \cdot {}^e\mathbf{T} - {}^e\mathbf{T} \cdot {}^{hi}\mathbf{D}$ as precision performance indexes. The errors \mathbf{T}_{eri} are shown in Tab. 1 for the proposed approach, i.e. the hybrid neural network and particle swarm optimization with the crossover and mutation (NNPSOwCM), and the least square method (LSM). It is shown that NNPSOwCM has higher precision than LSM.

5.3 Orthogonality analysis

The rotational matrix \mathbf{R} consists of three unit vectors \mathbf{n} , \mathbf{o} and \mathbf{a} , according to the least square method, the results of dot product of two elements in the estimated rotational matrix's are: $\mathbf{n}^T \mathbf{o} = 0,0086$, $\mathbf{o}^T \mathbf{a} = 0,0143$, and $\mathbf{a}^T \mathbf{n} = 0,0067$. According to the proposed approach, those are: $\mathbf{n}^T \mathbf{o} = -1,1102 \times 10^{-16}$, $\mathbf{o}^T \mathbf{a} = -2,2204 \times 10^{-16}$, and $\mathbf{a}^T \mathbf{n} = -1,9429 \times 10^{-16}$. As can be seen from the above analysis, the proposed approach that is NNPSOwCM can guarantee the orthogonality of the rotational matrix.

Table 1 Precision performance indexes of two methods

| | \mathbf{T}_{er1} | \mathbf{T}_{er2} | \mathbf{T}_{er3} |
|----------|--|--|--|
| NNPSOwCM | $\begin{bmatrix} 0,0032 & 0,0044 & 0,0023 & -0,1652 \\ 0,0014 & 0,0030 & -0,0008 & 0,5185 \\ -0,0006 & 0,0023 & -0,0058 & -0,2184 \\ 0 & 0 & 0 & 0 \end{bmatrix}$ | $\begin{bmatrix} -0,0026 & -0,0006 & -0,0010 & -0,1929 \\ -0,0007 & 0,0001 & 0,0023 & -0,2127 \\ -0,0008 & -0,0000 & 0,0014 & 0,2108 \\ 0 & 0 & 0 & 0 \end{bmatrix}$ | $\begin{bmatrix} 0,0041 & -0,0035 & 0,0041 & 0,0357 \\ 0,0040 & -0,0012 & -0,0051 & -0,0440 \\ 0,0011 & -0,0004 & 0,0012 & -0,2035 \\ 0 & 0 & 0 & 0 \end{bmatrix}$ |
| LSM | $\begin{bmatrix} -0,0023 & 0,0046 & 0,0028 & -0,5635 \\ 0,0012 & 0,0048 & -0,0056 & 0,1583 \\ -0,0005 & 0,0020 & -0,0059 & -0,1932 \\ 0 & 0 & 0 & 0 \end{bmatrix}$ | $\begin{bmatrix} -0,0076 & 0,0022 & 0,0007 & 0,6236 \\ -0,0011 & 0,0028 & -0,0022 & -0,4527 \\ -0,0011 & -0,0011 & 0,0038 & 0,1599 \\ 0 & 0 & 0 & 0 \end{bmatrix}$ | $\begin{bmatrix} -0,0091 & 0,0000 & 0,0071 & 0,1063 \\ -0,0019 & 0,0069 & -0,0206 & 0,2257 \\ 0,0061 & 0,0054 & -0,0051 & 0,4060 \\ 0 & 0 & 0 & 0 \end{bmatrix}$ |

6 Conclusions

In this paper, a new approach i.e. integrating neural network with rotational matrix and particle swarm optimization algorithm for the solution of the rotational components of the homogeneous transform of the hand-eye system is proposed, where the neural network is structured according to solving requirement of the rotational components of the homogeneous transform of the hand-eye relation. And an improved particle swarm optimization is adopted, where the crossover and mutation operation is used to update the velocity and position for particles, and the crossover probability is 1, and the inertia weight factor and the mutation probability is tuning adaptively according to the feature of particles' motion trajectory in longitudinal direction and lateral direction. So the relation of position and orientation of camera mounted in hand with respect to manipulator wrist is realized. Precision analysis shows that the proposed approach can meet the precision requirement in practice; and has advantages of simplicity and clarity, and guarantees the orthogonality of the three column vectors of estimated rotational matrix.

In the future, in the light of the feature of rotational matrix of camera's extrinsic parameters, we would like to develop a monocular vision system that makes the optical axis of camera be perpendicular to the test platform.

Acknowledgement

The work described in this paper is partially supported by National Natural Science Foundation of China under grant No. 51175187, National Hi-Tech Research and Development Program of China under grant No. 2007AA04Z111, and the Hunan Provincial Natural Science Foundation of China under grant No. 09JJ6092, and the Scientific Research Fund of Hunan Provincial Education Department under grant No. 09B092, and the Science & Technology Foundation of Guangdong Province under grant Nos. 2011B010100039, 2010B090400372, 2009B090300438 and 2009B090300251, and the Hunan Province colleges and Universities' Innovation platform open fund Projection (11K059). The authors would like to thank the reviewers for their constructive comments that improved the presentation of the paper.

7 References

- [1] Ganapathy, S. Decomposition of transformation matrices for robot vision, Int. Conf. on Robotics (Atlanta. GA. Mar, 1984), pp. 130-139.
- [2] Fischler, M. A.; Bolles, R. C. Random sample consensus: A paradigm for model fitting with applications to image analysis and automated cartography. // Commun. ACM, 24, 6(1981), pp. 381-395.
- [3] Gennery, D. B. Stereo-camera calibration, in Proc. Image Understanding Workshop, (1979), pp. 101-107.
- [4] Barnard, S. T.; Fischler, M. A. Computational stereo from an IU perspective. // Proc. Image Understanding Workshop, 1981, pp. 157-167.
- [5] Duda, R. O.; Nitzan, D.; Barrett, P. Use of range and reflectance data to find planar surface regions. // IEEE Transactions on Pattern Analysis and Machine Intelligence, Vol. PAMI-1, 3(1979), pp. 259-271.
- [6] Horaud, P.; Bolles, R. C. 3DPO's strategy to matching three-dimensional objects in range date. // Proc. Int. Conf. on Robotics (Atlanta. GA. Mar, 1984), pp. 78-85.
- [7] Nitzan, D.; Brain, A. E.; Duda, R. O. The measurement and use of registered reflectance and range data in sense analysis. // Proc. IEEE. Vol. 65, Feb. 1977, pp. 206-220.
- [8] Brown, M. K. Feature extraction techniques for recognizing solid objects with an ultrasonic range sensor. // IEEE Journal of Robotics and Automation. 1, 4(1985), pp. 191-205.
- [9] Grimson, W. E. L. Disambiguating sensory interpretation using minimal sets of sensory data. // Proc. IEEE Int. Conf. on Robotics and Automation (San. Francisco. CA. Apr. 1986), pp. 286-292.
- [10] Grimson, W. E. L.; Lozano-Perez, T. Model-based recognition and localization from sparse range or tactile data. // Int. J. Robotics Res. 3, 3(1984), pp. 248-255.
- [11] Fateh, M. M.; Fateh, S. Fine-tuning fuzzy control of robots. // Journal of Intelligent and Fuzzy Systems. 25, 4(2013), pp. 977-987.
- [12] Shiu, Y. C.; Ahmad, S. Calibration of wrist-mounted robotic sensors by solving homogenous Transform Equations of the form $AX=XB$. // IEEE Trans. on Robotics and Automation. 5, 10(1989), pp. 16-29.
- [13] Park, F.; Martin, B. Robot sensor calibration: Solving $AX = XB$ on the Euclidean group. // IEEE Transactions on Robotics and Automation (S1042-296X). 10, 5(1994), pp. 717-721.
- [14] Yang, G. L.; Kong, L. F.; Wang, J. A New Calibration Approach to Hand-Eye Relation of Manipulator. // Robot. 28, 4(2006), pp. 400-405.
- [15] Yuichi, Motai; Akio, Kosaka. Hand-eye calibration applied to viewpoint selection for robotic vision. // IEEE Transactions on Industrial Electronics. 55, 10(2008), pp. 3731-3741.
- [16] Zhang, X.; Li, A. G.; Ma, Z.; Hu, Y. Simultaneous calibration for relationship of robot hand-eye, based coordinates and world coordinates. // Control and Decision. 24, 10(2009), pp. 1531-1534.
- [17] Li, Mengxiang. Kinematic Calibration of an Active Head-Eye System. // IEEE Transactions on Robotics and Automation. 14, 1(1998), pp. 153-158.
- [18] Dornaika, F.; Horaud, R. Simultaneous Robot-World and Hand-Eye Calibration. // IEEE Transactions on Robotics and Automation. 14, 4(1998), pp. 617-622.
- [19] Ge, D. Y.; Yao, X. F.; Jiang, S. S.; Gu, Y. Z. On Hand-Eye Calibration of Manipulator with Orthogonal Neural Network and Genetic Algorithm. // ICIC Express Letters Part B: Applications. 2, 4(2011), pp. 899-904.
- [20] Fisher, W. D. The kinematic control of redundant manipulator. // Ph. D. dissertation, W. Lafayette: Purdue University, 1984.
- [21] Ngaopitakkul, A.; Jettanasen, C. Selection of Proper Activation Functions in Back-Propagation Neural Networks Algorithm for Identifying the Phase with Fault Appearance in Transformer Windings. // International Journal of Innovative Computing, Information and Control. 8, 6(2012), pp. 4299-4318.
- [22] Protasiewicz, J.; Szczepaniak, P. Neural Models of Demands for Electricity-Prediction and Risk Assessment. // Przeglad Elektrotechniczny (Electrical Review). 88, 6(2012), pp. 272-279.
- [23] Chen, S.; Hong, X.; Harris, C. J. Particle Swarm Optimization Aided Orthogonal Forward Regression for Unified Data Modeling. // IEEE Trans. on Evolutionary Computation. 14, 4(2010), pp. 477-499.
- [24] Liu, L. L.; Yang, S. X.; Wang, D. W. Particle Swarm Optimization with Composite Particles in Dynamic Environment. // IEEE Trans. on Systems, Man, and

- Cybernetics-Part B: Cybernetics. 40, 6(2010), pp. 1634-1648.
- [25] Shi, Y.; Eberhart, R. C. A modified swarm optimizer. // IEEE International Conference of Evolutionary Computation. (1998), pp. 69-73.
- [26] Mohamad, M. S.; Omatu, S.; Deris, S.; Yoshioka, M.; Ibrahim, Z. Selecting a Small Subset of Informative Genes from Gene Expression Data by Using a Modified Binary Particle Swarm Optimization. // International Journal of Innovative Computing, Information and control. 8, 6(2012), pp. 4285-4297.
- [27] Romić, K.; Galić, I.; Baumgartner, A. Character recognition based on region pixel concentration for license plate identification. // Tehnički Vjesnik - Technical Gazette. 19, 2(2012), pp. 321-325.
- [28] Zhao, Z. X.; Wen, G. J.; Zhang, X.; Li, D. R. Model-based Estimation for Pose, Velocity of Projectile from Stereo Linear Array Image. // Measurement Science Review. 12, 3(2012), pp. 104-110.
- [29] Hou, J. J.; Wei, X. G; Sun, J. H. Calibration Method for Binocular Vision Based on Matching Synthetic Images of Concentric Circles. // Acta Optica Sinica. 32, 3(2012), pp. 03150003-1-03150003-6.
- [30] Ge, D. Y.; Yao, X. F.; Xiang, W. J. Hand-Eye Calibration of Machine Vision System for Manipulator. // Applied Mechanics and Materials. 44-47, (2011), pp. 864-868.

Authors' addresses**Dong-Yuan Ge**

Department of Mechanical and Energy Engineering, Shaoyang University, Shaoyang 422004, Hunan, China
+8615080900986, E-mail: gordon399@163.com
School of Mechanical and Automotive Engineering, South China University of Technology, Guangzhou, 510640, Guangdong China

Xi-Fan Yao

School of Mechanical and Automotive Engineering, South China University of Technology, Guangzhou, 510640, Guangdong China

Qing-He Yao

Department of Mechanical Engineering, Faculty of Engineering, Kyushu University, 744, Motooka, Nishi-ku, Fukuoka 819-0395, Japan

Hong Jin

School of Mechanical and Automotive Engineering, South China University of Technology, Guangzhou, 510640, Guangdong China



©Ali AlEsfain

Location

Istanbul, where Asia and Europe meet across the Bosphorus, is a unique city in terms of its history and strategic importance. Founded nearly 3,000 years ago as Byzantium, the city was the intellectual and cultural centre of the Western world following the decay of Rome. Istanbul persists as a city of contrasts and the crossroad of many different cultures. This is reflected in its heritage architecture, including

Submission Information

Papers are invited on the topics outlined and others falling within the scope of the meeting. Abstracts of no more than 300 words should be submitted as soon as possible.

Abstracts should clearly state the purpose, results and conclusions of the work to be described in the final paper. Final acceptance will be based on the full-length paper, which if accepted for publication must be presented at the conference.

The language of the conference will be English.

Online submission:
wessex.ac.uk/disaster2015

Email submission:
gwest@wessex.ac.uk

Submit your abstract with 'Disaster Management 2015' in the subject line.
Please include your name, full address and conference topic.

the renowned Hagia Sophia, a series of breath-taking mosques such as that of Suleiman the Magnificent built by Architect Sinan (1489-1588), and the Blue Mosque built by the famous Architect Sedefkar Mehmet Aga, who was a student of Great Sinan, the master of the domes who innovated many aspects of Ottoman Design. Sinan's influence on Ottoman Empire architecture in the 16th century was fundamental. His courtly works shaped the whole panoramic view of Istanbul.

Other significant Ottoman buildings in Istanbul include Topkapi residence of the sultans and their harems. Amongst the hidden sites to visit are the ancient Byzantine underground cisterns which have been beautifully restored.

It is impossible to describe the immense cultural and architectural wealth of Istanbul in a few paragraphs, with its numerous museums, ancient ruins, fantastic food, and the friendliness of its inhabitants.

Conference Venue

The Taşkışla building, consisting of large corridors around a beautiful courtyard, has recently been completely restored by the Dean of Administration at ITU. It has comfortable auditoria with excellent audio visual facilities.

The building is within the centre of town and well located in the Taksim Square area, with the Grand Hyatt Hotel across the road from its main entrance. There are many other hotels within walking distance with a range of services and price variations to suit all conference delegates.

Conference Secretariat

Genna West

gwest@wessex.ac.uk

Wessex Institute
Ashurst Lodge, Ashurst
Southampton, SO40 7AA, UK

Tel: +44 (0) 238 029 3223
Fax: +44 (0) 238 029 2853

For more information visit:
wessex.ac.uk/disaster2015



CALL FOR PAPERS

DISASTER MANAGEMENT 2015

4th International Conference on Disaster Management and Human Health: Reducing Risk, Improving Outcomes

20 - 22 May 2015
Istanbul, Turkey

Organised by

Wessex Institute, UK
Faculty of Architecture, Istanbul Technical University, Turkey



wessex.ac.uk/disaster2015

Sponsored by

WIT Transactions on the Built Environment
International Journal of Safety and Security Engineering
AFAD - Turkish Prime Minister Disaster and Emergency Management Authority

Benefits of Attending

Conference Proceedings Papers presented at Disaster Management 2015 will be published by WIT Press in Volume 150 of WIT Transactions on the Built Environment (ISSN: 1746-4498 Digital ISSN: 1743-3509). WIT Press ensures maximum worldwide dissemination of your research through its own offices in Europe and the USA, and via its extensive international distribution network.

Delegates will have the choice of receiving the conference book as either hard cover or digital format on a USB flash drive. The USB flash drive will, in addition, contain papers from previous conferences in this series.

Indexing and Archiving Papers presented at Wessex Institute conferences are referenced by CrossRef and regularly appear in notable reviews, publications and databases, including referencing and abstracting services such as SCOPUS, Compendex, Thomson Reuters Web of Knowledge and ProQuest. All conference books are archived in the British Library and American Library of Congress.

Digital Archive All conference papers are archived online in the WIT eLibrary (<http://library.witpress.com>) where they are easily and permanently available to the international scientific community.

Journal Papers After the conference, presenters at Disaster Management 2015 will be invited to submit an enhanced version of their research for possible publication in the International Journal of Safety and Security Engineering published by the Wessex Institute.

Reviews Abstracts and papers are reviewed by members of the International Scientific Advisory Committee and other experts.

Open Access Open Access allows for the full paper to be downloaded from the WIT eLibrary archives, offering maximum dissemination. Authors who choose this option will also receive complimentary access for one year to the entire WIT eLibrary.

Reduced Fee for PhD Students The Wessex Institute believes in the importance of encouraging PhD students to present and publish innovative research at their conferences. As a result, the Institute offers PhD students a much reduced conference fee.

Citations When referencing papers presented at this conference please ensure that your citations refer to **Volume 150 of WIT Transactions on the Built Environment** as this is the title under which papers appear in the indexing services.

Conference Chairmen

S M Sener
Istanbul Technical University, Turkey

C A Brebbia

Wessex Institute, UK

O Ozcevik
Istanbul Technical University, Turkey

International Scientific Advisory Committee

E Chu
National Yunlin University of Science and Technology, Taiwan

R Ernsteins
University of Latvia, Latvia

V Ferrara
University of Rome 'La Sapienza', Italy

F Gardia
University of Rome 'La Sapienza', Italy

C Gociman
University of Architecture & Urban Planning, Romania

S Hernandez
University of A Coruña, Spain

S Kundak
Istanbul Technical University, Turkey

F T Lin
National Cheng-Kung University, Taiwan

I Malkina-Pykh
Russian Academy of Sciences, Russia

D Mirel
Florida State University, USA

D Novelo-Casanova
Universidad Nacional Autonoma de Mexico, Mexico

F Oktay
Disaster and Emergency Management Presidency (AFAD), Turkey

O Renn
University of Stuttgart, Germany

M Takezawa
Nihon University, Japan

Local Scientific Committee

E Acar
Istanbul Technical University, Turkey

Y Demir
Istanbul Greater Municipality, Turkey

F Gezici Korten
Istanbul Technical University, Turkey

I Helvaciglu
Istanbul Technical University, Turkey

A Ilik
Istanbul Technical University, Turkey

M Kadoglu
Istanbul Technical University, Turkey

N Okay
Istanbul Technical University, Turkey

A Tezer
Istanbul Technical University, Turkey

N Torunbali
Istanbul Technical University, Turkey

H Turkoglu
Istanbul Technical University, Turkey



The fourth International Conference on Disaster Management is being reconvened following the success of the previous three meetings, held at the Wessex Institute in the New Forest, UK in 2009, the University of Central Florida in Orlando, USA in 2011 and A Coruña, Spain in 2013.

This series of conferences originated with the need for academia and practitioners to exchange knowledge and experience on the way to handle the increasing risk of natural and human-made disasters. Recent major earthquakes, tsunamis, hurricanes, floods and other natural phenomena have resulted in huge losses in terms of human life and property destruction. A new range of human-made disasters have afflicted humanity in modern times; terrorist activities have been added to more classical disasters such as those due to the failure of industrial installations for instance.

It is important to understand the nature of these global risks to be able to develop strategies to prepare for these events and plan effective responses in terms of disaster management and the associated human health impacts.

The conference provides a forum for the exchange of information between academics and practitioners, and a venue for presentation of the latest developments. The corresponding volume of WIT Transactions on the Built Environment containing the papers presented at the meeting has been published in paper and digital format and widely distributed around the world. The papers are also archived in the WIT library (<http://library.witpress.com>) where they are available to the international community.

Taşkışla Building

The conference will take place at the Taşkışla Building, which houses the Faculty of Architecture at Istanbul Technical University.

Istanbul Technical University was established in 1773 under its original name of the Royal School of Naval Engineering. It was responsible for training marine cartographers and ship builders. In 1795 the Royal School of Military Engineering was established to educate technical staff of the army. Architecture education was introduced to the school in 1847.

In 1883 it became the "Engineering Academy", teaching essential skills needed in planning and implementing the country's new infrastructure projects. Gaining university status in 1928, the Engineering Academy continued to provide education in the fields of engineering and architecture until it was incorporated into Istanbul Technical University (ITU) in 1944, and in 1946 ITU became an autonomous university which included faculties of architecture, civil engineering, mechanical engineering, and electrical and electronic engineering.

With a history stretching back nearly 250 years and providing technical knowledge within a modern educational environment and excellent academic staff, ITU is strongly identified with architectural and engineering education in Turkey. Since its foundation, ITU has constantly led the way in reform movements.

Conference Topics

- Disaster analysis
- Disaster monitoring and mitigation
- Emergency preparedness
- Risk mitigation
- Risk and security
- Safety and resilience
- Socio-economic issues
- Health risk
- Case studies
- Human factors
- Multihazard risk assessment